ELSEVIER

Signal Processing 79 (1999) 15–28

SIGNAL PROCESSING

www.elsevier.nl/locate/sigpro

Time–frequency analysis of multiple resonances in combustion engine signals

LJubiša Stanković[1,*], Johann F. Böhme

Signal Theory Group, Ruhr University Bochum, 44780 Bochum, Germany

Received 4 June 1998; received in revised form 17 May 1999

Abstract

This paper presents time–frequency analysis of multiple resonances in combustion chamber pressure signals and corresponding structure-born sound signals of the cylinder block of a combustion engine considering only one combustion cycle. Since the Wigner distribution proved itself as a good tool for these kinds of signals, the requirement which we imposed here was to produce a sum of the Wigner distributions of the signal components separately, but without cross-terms using only one signal realization. A distribution having this property can be achieved using the S-method. Based on this property of the method, we investigate a procedure to estimate the instantaneous frequencies that are functions of temperature within the combustion chamber and the energies of the components that are used for knock detection. The calculation delay is smaller than the duration of one combustion cycle. This can provide an efficient and accurate combustion control of spark-ignition car engines. The procedure is demonstrated on several simulated and experimental signals.

Zusammenfassung

Dieser Artikel präsentiert die Zeit–Frequenz Analyse mehrfacher Resonanzen von Drucksignalen in Brennkammern und den korrespondierenden Körperschallsignalen des Zylinderblocks eines Verbrennungsmotors unter Berücksichtigung nur eines Verbrennungszyklus. Da die Wigner Verteilung sich als geeignetes Werkzeug für diese Art von Signalen erwiesen hat, verlangen wir als Anforderung die Berechnung der Summe der Wigner Verteilungen der einzelnen Signalkomponenten, jedoch ohne die Kreuzterme und unter Benutzung nur einer Realisierung des Signals. Eine Verteilung mit dieser Eigenschaft kann über der S-Methode erhalten werden. Auf Grund dieser Eigenschaft der Methode untersuchen wir ein Verfahren zur Schätzung der Momentan-frequenzen. Diese Frequenzen sind Funktionen der Temperatur innerhalb der Brennkammer und der Energien der Komponenten die für die Klopfdetektion verwendet werden. Die Verzögerung aufgrund der Berechnung ist kleiner als die Dauer eines Verbrennungszyklus. Dies erlaubt eine effiziente und genaue Verbrennungsregelung von Automotoren. Die Prozedur wird anhand verschiedener simulierter und experimenteller Signale vorgeführt.

Résumé

Cet article présente une analyse temps–fréquence de résonances multiples dans des signaux de pression de chambres de combustion, et des signaux correspondants de sons des structures du bloc de cylindres d'un moteur à combustion, en ne

* Corresponding author. Fax: + 49-00381-81-244921.

E-mail address: sta@sth.ruhr-uni-bochum.de (LJubiša Stanković)

[1] On leave from the University of Montenegro, Montenegro. Supported by the Alexander von Humboldt foundation.

0165-1684/99/$ - see front matter
PII: S0165-1684(99)00077-8

considérant d'un seul cycle de combustion. Comme la distribution de Wigner s'est révélée être un bon outil pour ces types de signaux, l'exigence que nous nous sommes imposée ici est de produire une somme de distributions de Wigner des composants des signaux séparément, mais sans termes croisés, en utilisant seulement une réalisation du signal. Une distribution ayant cette propriété peut être atteinte en utilisant la méthode S. Sur la base de cette propriété de la méthode, nous avons étudié une procédure d'estimation des fréquences instantanées qui sont fonctions de la température dans la chambre de combustion et des énergies des composants qui sont utilisés pour la détection des chocs. Le retard de calcul est inférieur à la durée d'un cycle de combustion. Ceci peut fournir un contrôle de combustion efficace et précis pour des moteurs de voitures à allumage par étincelle. La procédure est démontrée sur plusieurs signaux simulés et expérimentaux.

Keywords: Time–frequency analysis; Combustion engine signals; Wigner distribution; Instantaneous frequency; Knock

1. Introduction

Structure-borne sound signals and more seldom pressure signals are used for efficient combustion control of spark-ignition engines. This control can increase efficiency, reduce pollution and noise, and protect against knock. Knock is an abnormal combustion that causes rapid rise of the temperature and pressure. Its detection is an important problem since frequent knock occurrence can destroy the engine or significantly degrade its performances. By measuring the pressure at a suitable point inside the cylinder we can observe the combustions. However, pressure sensors are expensive, difficult to mount and not robust enough. These are the reasons why their application is mainly limited to test beds. Sound signals can be considered as time-varying filtered versions of the pressure and can be used for the observation of diagnostic parameters, as resonance frequencies that are function of temperature, and resonance energies that indicate knock [4,8,13–15,25]. The application of acceleration sensors on the surface of the engine is easy and economical, but sound signals are superimposed with mechanical noise that can significantly influence the analysis.

Such sound and pressure signals are highly nonstationary, therefore neither classical signal analysis tools in time-domain nor in frequency-domain are efficient here. Even the short-time Fourier transform and its energetic version spectrogram, as extensions of the Fourier analysis to the nonstationary problems, cannot be used due to high nonstationary effects in the car engine signals [15]. These signals require joint time–frequency analysis [4,5,7,8,13–15,18]. This approach to the car engine signal analysis was introduced in [18]. It has been shown that pressure signals and sound signals can be considered as frequency modulated multicomponent signals with random amplitudes and phases of the components when low frequency parts are neglected [3,9,13–15]. Due to cyclostationarity and the property that the components of these signals are mutually not correlated, it has been found that the Wigner distribution can be used as an efficient time–frequency tool for their analysis [13–15]. The problem of cross-terms in the Wigner distribution was resolved by averaging over-pressure or sound signals of different combustion cycles of the engine under similar working conditions. Since the components are not correlated, the cross-terms disappear and theoretically, using an infinite number of combustions, the mean of Wigner distributions converges to the Wigner–Ville spectrum containing the auto-terms only. Time–frequency representation concentration can be improved using the Weyl spectrum introduced in [17]. An extensive study, based on the Wigner distribution, with numerous results and conclusions has been reported [14,15]. The main disadvantage of this approach is that the elimination of cross-terms requires a large number of combustions meaning a long observation time and can mask the effects in a single combustion or a decision based on the analysis can be too late.

The aim of this paper is to present a time–frequency analysis of car engine sound or pressure signals based on a single combustion. Since the Wigner distribution proved itself as a good tool for these kind of signals, the requirement which we

impose here was to produce a sum of the Wigner distributions of the signal components separately, but without cross-terms using only one signal realization. A distribution having this property has been introduced in [19] referred to as the S-method and studied in [20–22]. A hardware realization of the S-method is presented in [23]. Its comparison with other reduced interference distributions for the linear frequency modulated signals is done in [21]. Based on the nice property of this method that it can produce the sum of the Wigner distributions of all signal components, we shall be able to estimate the powers and instantaneous frequencies of each sound or pressure signal component, that is the main goal of this paper. Knowing the instantaneous power, we can calculate the energy of components and make a decision if a knocking combustion occurred or not [14,15]. This can provide efficient and accurate information for anti-knock control of spark-ignition engines.

The paper is organized as follows. A model of the car engine signals is presented in Section 2. Its time–frequency analysis is studied in Section 3. The S-method as a tool for time–frequency analysis is reviewed in this section, as well. The discrete forms of the presented algorithms are given. Section 4 contains synthetic and real signals examples and discussions.

2. Car engine signal models and analysis

A pressure signal or an undisturbed sound signal can be described by a multicomponent frequency and amplitude modulated signal if low frequency parts of the signals are filtered out [3,9,13–15]. Consider first a very simple form of a real mono-component signal neglecting cyclostationarity,

$$\bar{y}(t) = 2A(t)\cos(\varphi(t)), \tag{1}$$

with $\varphi(t) = \omega_0 \int_{-\infty}^{t} m(\tau)\,\mathrm{d}\tau + \Phi$, where $\omega_0 m(t)$ is the instantaneous frequency and Φ is a random phase. If we suppose that the variations of amplitude are much slower than the phase variations, then the analytic signal of $\bar{y}(t)$ can be written as

$$y(t) = A(t)\mathrm{e}^{\mathrm{j}\varphi(t)}. \tag{2}$$

The pseudo-Wigner distribution

$$\mathrm{WD}_{yy}(t,\omega) = \int_{-\infty}^{\infty} w\left(\frac{\tau}{2}\right) w\left(-\frac{\tau}{2}\right) y\left(t+\frac{\tau}{2}\right) \times y^{*}\left(t-\frac{\tau}{2}\right)\mathrm{e}^{-\mathrm{j}\omega\tau}\,\mathrm{d}\tau \tag{3}$$

provides a time–frequency representation of the signal $y(t)$. Two important properties of the pseudo-Wigner distribution that will be used here are [10]

$$\frac{1}{2\pi}\int_{-\infty}^{\infty} \mathrm{WD}_{yy}(t,\omega)\,\mathrm{d}\omega = A^2(t), \tag{4}$$

$$\frac{\int_{-\infty}^{\infty} \omega \mathrm{WD}_{yy}(t,\omega)\,\mathrm{d}\omega}{\int_{-\infty}^{\infty} \mathrm{WD}_{yy}(t,\omega)\,\mathrm{d}\omega} = \varphi'(t) = \omega_0 m(t). \tag{5}$$

These properties hold for any signal $y(t)$, as far as $w(0) = 1$.

In the case of linear frequency modulated signals, if the variations of $A(t \pm \tau)$ within $w(\tau)$ are much slower than the phase variations, the pseudo-Wigner distribution can be written as

$$\mathrm{WD}_{yy}(t,\omega) = A^2(t)W(\omega - \varphi'(t)) = A^2(t)W(\omega - \omega_0 m(t)),$$

where $W(\omega)$ is the Fourier transform of $w(\tau/2)w(-\tau/2)$. The instantaneous frequency can be now obtained using

$$\varphi'(t) = \arg\left\{\max_{\omega} \mathrm{WD}_{yy}(t,\omega)\right\}, \tag{6}$$

if $W(\omega)$ reaches its maximum at $\omega = 0$.

If the instantaneous frequency is not a linear function of time, we have either to use the general unbiased form (5) or to use the simple form (6) being aware that a biased value may be obtained. The maximal possible value of the bias would be $|\varphi'(t) - \arg\{\max_{\omega} \mathrm{WD}_{yy}(t,\omega)\}| \leqslant \frac{1}{6} M_2 C$, where M_2 is the supremum of the instantaneous frequency second derivative, $M_2 = \sup|\varphi^{(3)}(t)|$, and C is a constant, $C = -W^{(2)}(0)/W^{(4)}(0)$ with $W^{(2)}(0)$ and $W^{(4)}(0)$ being the second- and the fourth-order derivatives of $W(\omega)$ at $\omega = 0$. For a rectangular window $C = \frac{3}{20} T_w^2$, where T_w is the width

of the window $w(\frac{1}{2}\tau)w(-\frac{1}{2}\tau)$, [12]. For $M_2 \ll \frac{1}{6}C$, $\arg\{\max_\omega \mathrm{WD}_{yy}(t,\omega)\} \simeq \varphi'(t)$ holds.

Therefore, if we know the pseudo-Wigner distribution of a monocomponent frequency modulated signal, we can exactly reconstruct its amplitude and instantaneous frequency either by using Eq. (6) or, if the nonlinearities in the instantaneous frequency are high, by using Eq. (5).

In reality, sound and pressure signals should be modeled as multicomponent signals [3,9,13–15]. The analysis slightly complicates in this case. Consider a signal

$$\bar{y}(t) = 2\sum_{p=1}^{P} A_p(t)\cos(\varphi_p(t)),$$

with

$$\varphi_p(t) = \omega_p \int_{-\infty}^{t} m_p(\tau)\,\mathrm{d}\tau + \Phi_p, \quad p = 1,2,\ldots,P,$$

where $\omega_p m_p(t)$ are the instantaneous frequencies and Φ_p are the random phases of the components $p = 1,2,\ldots,P$. The problem would be resolved if we were able to use a distribution having the property

$$D(t,\omega) = \sum_{p=1}^{P} \mathrm{WD}_{y_p y_p}(t,\omega), \tag{7}$$

where $\mathrm{WD}_{y_p y_p}(t,\omega)$ is the pseudo-Wigner distribution of the component $y_p(t)$, correspondingly.

Note. If a large number of realizations of a stochastic process $y(t) \cong \sum_{p=1}^{P} y_p(t)$ were known and if the components were uncorrelated, $E\{y_p(n)y_q^*(m)\} = 0$, $p \neq q$, then averaging the Wigner distribution, or the product $y(t+\frac{1}{2}\tau)y(t-\frac{1}{2}\tau)$, using realizations from different combustions, would produce Eq. (7), [3,13,14]. However, if we want signal processing based on a single realization of $y(t)$, then this approach is not applicable.

A method that produces the distribution having the property that it is equal to the sum of the pseudo-Wigner distributions of each signal component in the case of multicomponent signals was introduced as the S-method [19–23]. It will be shortly reviewed in the sequel.

3. The S-method and car engine signals parameters estimation

A definition of the short-time Fourier transform (STFT) of the signal $y(t)$, with a finite duration window $w(\tau)$, is

$$\mathrm{STFT}_y(t,\omega) = \int_{-\infty}^{\infty} y(t+\tau)w(\tau)\mathrm{e}^{-\mathrm{j}\omega\tau}\,\mathrm{d}\tau. \tag{8}$$

It is easy to establish the relationship between Eq. (8) and Eq. (3). It has been derived in [19] as

$$\mathrm{WD}_{yy}(t,\omega) = \frac{1}{\pi}\int_{-\infty}^{\infty} \mathrm{STFT}_y(t,\omega+\theta) \times \mathrm{STFT}_y^*(t,\omega-\theta)\,\mathrm{d}\theta. \tag{9}$$

This relation has led to the S-method definition [19–21,23]:

$$\mathrm{SM}(t,\omega) = \frac{1}{\pi}\int_{-\infty}^{\infty} P(\theta)\mathrm{STFT}_y(t,\omega+\theta) \times \mathrm{STFT}_y^*(t,\omega-\theta)\,\mathrm{d}\theta, \tag{10}$$

where $P(\theta)$ is a finite frequency-domain window, we also assume to be rectangular, $P(\theta) = 0$, for $|\theta| > L_P$. The width L_P may be time and frequency dependent, as well. The S-method belongs to the general Cohen class of distributions [6]. It can produce the desired representation of a multicomponent signal such that the distribution of each component is its pseudo-Wigner distribution, avoiding cross-terms.

Consider the signal $y(t) = \sum_{p=1}^{P} y_p(t)$, where $y_p(t)$ are monocomponent signals. Assume that the absolute value of the short-time Fourier transform of each component is greater than an assumed small reference level R only inside the region $D_p(t,\omega)$, $p = 1,2,\ldots,P$. Denote the length of the pth region along ω, for a given t, by $2B_p(t)$, and its central frequency by $\omega_{0p}(t)$. The S-method of $y(t)$ produces approximately the sum of the pseudo-Wigner distributions $\mathrm{WD}_{y_p y_p}(t,\omega)$ of each signal component,

$$\mathrm{SM}_{yy}(t,\omega) \cong \sum_{p=1}^{P} \mathrm{WD}_{y_p y_p}(t,\omega), \tag{11}$$

if the regions $D_p(t,\omega)$, $p = 1,2,\ldots,P$, do not overlap for $p \neq q$, and if the width of the rectangular window $P(\theta)$, for a point (t,ω), is defined by

$$L_P(t,\omega) = \begin{cases} B_p(t) - |\omega - \omega_{0p}(t)|, & \text{for } (t,\omega) \in D_p(t,\omega), \\ & p = 1,2,\ldots,P, \\ 0 & \text{elsewhere.} \end{cases} \quad (12)$$

The proof of this statement is evident since Eqs. (9) and (10) produce the same value for each signal component individually provided that the proposition assumptions hold.

Note. Any window $P(\theta)$ with constant width $L_P \geqslant \max_{\omega,t}\{L_P(\omega,t)\}$ produces $\mathrm{SM}_{yy}(t,\omega) \cong \sum_{p=1}^{P} \mathrm{WD}_{y_p y_p}(t,\omega)$, if the regions $D_p(t,\omega)$, $p = 1,2,..,P$, are at least $2L_P$ apart along the frequency axis, i.e., $|\omega_{0p}(t) - \omega_{0q}(t)| > B_p(t) + B_q(t) + 2L_P$, for each p, q and t. This is the S-method with constant window width, as it was originally introduced in [19,20].

3.1. Discrete forms

For the signal $y(t)$ sampled with sampling interval T and N samples within the window $w(\tau)$, the discrete form of Eq. (10), denoted by $\mathrm{SM}(n,k) = \mathrm{SM}(nT,(2\pi/NT)k)$, is

$$\mathrm{SM}(n,k) = \frac{2}{NT} \sum_{i=-L_P(n,k)}^{L_P(n,k)} \mathrm{STFT}(n,k+i) \times \mathrm{STFT}^*(n,k-i), \quad (13)$$

where

$$\mathrm{STFT}(n,k) = T \sum_{m=-N/2}^{N/2-1} w(mT)y(nT+mT)\mathrm{e}^{-\mathrm{j}(2\pi/N)mk} \quad (14)$$

is the discrete form of the short-time Fourier transform (STFT). Note that $T_w = NT$ is the duration of the window $w(\tau)$. Very efficient methods for the STFT realizations by using either the FFT algorithms or the recursive approaches are well known [1,2,16,19,23].

After the STFT is obtained, the numerical realization of the S-method (13) is very simple according to

$$\mathrm{SM}(n,k) = \frac{2}{NT}\left(\mathrm{SPEC}(n,k) + 2\sum_{i=1}^{L_P(n,k)} \Re[\mathrm{STFT}(n,k+i)\mathrm{STFT}^*(n,k-i)]\right), \quad (15)$$

where $\mathrm{SPEC}(n,k) = |\mathrm{STFT}(n,k)|^2$ denotes the spectrogram, while the other terms in the summation (15) improve its concentration to the Wigner distribution quality.

There are two possibilities to implement this summation:

1. With a signal independent $L_P(n,k) = L_P$. This way is very simple, and from our experience very efficient.
2. With a signal dependent $L_P(n,k)$ the summation lasts until zero value of $\mathrm{STFT}(n,k+i)$ or $\mathrm{STFT}(n,k-i)$ is detected for each point (n,k). Practically, that means a square absolute value of $\mathrm{STFT}(n,k+i)$ or $\mathrm{STFT}(n,k-i)$ smaller than a reference level R^2.

3.2. Determination of the regions of support and reference level

In order to perform the integrations over the region D_p within the pth component, we have to find that region. Its determination will be based on an assumed reference level R^2. For a given time instant n, the frequency range of a region D_p denoted by $D_{p|n}$ is determined as a set of neighboring points where the S-method (or the spectrogram) is absolutely greater than the assumed reference level. We have assumed that the interval $D_{p|n}$ ends when two subsequent points are below the reference level R^2. For the analysis of car engine signals we have found the reference level defined as a fraction of the signal power

$$R_n^2 = \frac{1}{Q^2} \sum_{k=-N/2}^{N/2-1} \mathrm{SM}(n,k) \quad (16)$$

rather than a fraction of the distribution's maximal values as very convenient for the determination of

$D_{p|n}$ in Eqs. (17) and (18). This helped to avoid the summation over the regions where a small signal energy is almost uniformly distributed over the wide frequency interval and a given time instant n.

For numerical examples, computational efficiency, and specific implementations see [19–23].

3.3. Parameters of a discrete signal estimation

After the S-method is calculated using either signal independent or signal dependent L_P in Eq. (15), and the regions of support D_p, i.e. frequency intervals $D_{p|n}$ using R^2 are found for each component, then the signal's squared amplitude is calculated as

$$A_p^2(n) = \frac{1}{NT} \sum_{k \in D_{p|n}} \mathrm{SM}_{yy}(n,k), \quad p = 1,2,\ldots,P. \tag{17}$$

For linear frequency modulated signal components the instantaneous frequencies are obtained using

$$\begin{aligned} k_p(n) &= \arg\left\{ \max_{k \in D_{p|n}} \mathrm{SM}_{yy}(n,k) \right\}, \quad p = 1,2,\ldots,P, \\ \varphi_p'(n) &= \frac{2\pi}{NT} k_p(n). \end{aligned} \tag{18}$$

For a simpler graphical presentation of the results, the amplitude value $A_p^2(n)$ is assigned to the point $(n, k_p(n))$ in the time–frequency plane (n,k). A new matrix

$$A_M(n,k) = \begin{cases} A_p^2(n) & \text{for } (n,k) = (n,k_p(n)), \\ 0 & \text{elsewhere,} \end{cases} \tag{19}$$

is formed to that aim. It has zero values everywhere except for the points $(n,k_p(n))$. The matrix $A_M(n,k)$ contains full information about the instantaneous frequencies and powers and allow an easy presentation and energy calculation. The pth resonance energy is defined and estimated by

$$\begin{aligned} E_p &= \int_{-\infty}^{\infty} |y_p(t)|^2 dt = \int_{-\infty}^{\infty} A_p^2(t)\,\mathrm{d}t \\ &= \frac{1}{2\pi} \int_{-\infty}^{\infty} \int_{\omega \in D_{p|t}} \mathrm{SM}_{yy}(t,\omega)\,\mathrm{d}\omega\,\mathrm{d}t \\ &\cong \sum_{n=-\infty}^{\infty} A_p^2(n) T, \end{aligned} \tag{20}$$

where Eq. (17) is used. The summation over n is done within a signal component. The practical realization of this summation is performed using the matrix $A_M(n,k)$. At each following time instant n, the non-zero value of $A_M(n,k)$ placed according to Eq. (19) at $(n,k_p(n))$ is summed with the non-zero value from the previous time instant $(n-1)$ if they belong to the same signal component. The indicator of the points $(n,k_p(n))$ and $(n-1,k_p(n-1))$ belonging to the same component is the intersection of the corresponding regions of support $D_{p|n}$ and $D_{p|n-1}$. If these regions overlap along the frequency axis, we say that they belong to the same component.

The decision if two points $(n,k_p(n))$ and $(n-1,k_p(n-1))$ belong to the same component can be also based on a simple analysis as follows. If the points in the time–frequency plane are enough dense and we assume that the instantaneous frequencies are smooth functions, then we may say that the points $(n,k_p(n))$ and $(n-1,k_p(n-1))$ belong to the same signal component if they are within a defined range along the frequency axis, for example if $|k_p(n) - k_p(n-1)| \leqslant b$, i.e., if the instantaneous frequencies do not absolutely change for more than b frequency axis steps during one time axis step. Note that too small b would cause that if the condition $|k_p(n) - k_p(n-1)| \leqslant b$ is not satisfied for a given component p and instant n, then the algorithm stops summation (20) at instant n and consider the remaining part of the pth component as a new component with respect to energy calculation. Too large b can cause that the instantaneous frequencies of more than one component satisfy $|k_p(n) - k_p(n-1)| \leqslant b$. For engine signals, $b = 2$ is appropriate.

The estimation of amplitude and instantaneous frequency is influenced by the input noise. Variance of the amplitude estimate, according to Eq. (17), may be obtained using the results from [24], as $\sigma_{A^2}^2 = 4K\sigma_n^2(2A^2(n) + \sigma_n^2)E_w/N^2$, where E_w is the energy of the lag window, σ_n^2 is the input noise variance, and K is the number of samples within $D_{p|n}$ for a given n. For small noise, the ratio $\sigma_{A^2}^2/A^2(n) \cong 8K(E_w/N^2)(\sigma_n^2/A^2(n))$ is proportional to the input signal-to-noise-ratio. With a large value of N, this ratio is very small. Variance of the instantaneous frequency estimate (18), due to the

input noise, is given by $\sigma_{\omega}^2 \cong (\sigma_n^2/2A^2(n))G_w(1/N^2T)$, where G_w is a constant depending on the window type only [12]. Details on the estimation accuracy may be found in [12,24,11].

4. Examples and results discussion

4.1. Synthetic car engine signals

The presented procedure is tested first on a synthetic five component signal with linear frequency modulated components

$$y(t) = 2\sum_{p=1}^{5} A_p(t)\cos(\varphi_p(t)) + n(t), \tag{21}$$

where

$$\varphi_p(t) = c_{p2}t^2 + c_{p1}t + \Phi_p,$$

$$A_p(t) = \begin{cases} A_p t e^{-d_p t}, & t \geqslant 0, \\ 0 & \text{elsewhere}, \end{cases}$$

$$p = 1,2,\ldots,P. \tag{22}$$

Wideband Gaussian noise with standard deviation σ_n is denoted by $n(t)$, while the random phases Φ_p are uniformly distributed within $[0,2\pi]$. We assumed that the signal (21) begins at $t = 0$ and its main part is located within normalized unity time period $0 \leqslant t \leqslant 1$. Observation period was then widened to $-0.1 \leqslant t \leqslant 1.5$. The sampling interval was $T = 1/256$. The Hanning window $w(\tau)$ was used. Its width was $T_w = NT = 1$ with $N = 256$ samples, as well as $\sigma_n = 0.1$. Signal parameters A_p, d_p, c_{p2}, c_{p1} are given in Table 1.

The signal defined by Eqs. (21)–(22) with parameters given in Table 1 is presented in Fig. 1(a). Using this signal we calculated the S-method with $L_P = 4$ (Fig. 1(e)). Time–frequency representation produced by the S-method is compared with two other basic time–frequency distributions: the Wigner distribution and the spectrogram. As it is known the Wigner distribution suffers from the cross-terms. In the case of a five component signal there are 10 cross-terms, many of them overlapping each other and overlapping signal components (Fig. 1(c)). The spectrogram is shown in Fig. 1(b). Its resolution is quite low and, as it has been shown in [15] for these kind of signals, cannot be significantly improved by changing the window $w(\tau)$ form. Fig. 1(d,e) visually confirm Eq. (11). The S-method (Fig. 1(e)) produces the distribution that is equal to the sum of the Wigner distributions calculated for each signal component separately (Fig. 1(d)). The calculation of distribution presented in Fig. 1(d) is possible since in the simulation, and only in the simulation, we know the signal components separately. The S-method comparison with other reduced interference distributions from the Cohen class in the case of the linearly frequency modulated signals is performed in [21].

After the S-method is obtained, the instantaneous frequencies, powers and energies as cumulative powers of each signal component are calculated according to relations (17)–(20) (see Fig. 1(f,g,h)). Reference level in Eq. (16) was $Q^2 = 200$. The method's accuracy is checked by comparing the obtained values with the exact instantaneous frequencies, powers and energies, presented in Fig. 1(f,g,h) by lines. The agreement is very high. Note that a small deviation of the estimated instantaneous frequency from the exact one exists at the very beginning of each signal component, $t = 0$. This can be explained by the fact that here the amplitude variations are very fast and the assumption that the signal is linearly frequency modulated does not hold here.

Table 1
Signal parameters

p	1	2	3	4	5
A_p	12	8	6	4	6.5
d_p	8	6	6	5	5.8
c_{p_2}	$-12\sqrt{2}\pi$	$-12\sqrt{2}\pi$	$-12\sqrt{2}\pi$	$-12\sqrt{2}\pi$	$-12\sqrt{2}\pi$
c_{p_1}	36π	76π	116π	156π	196π

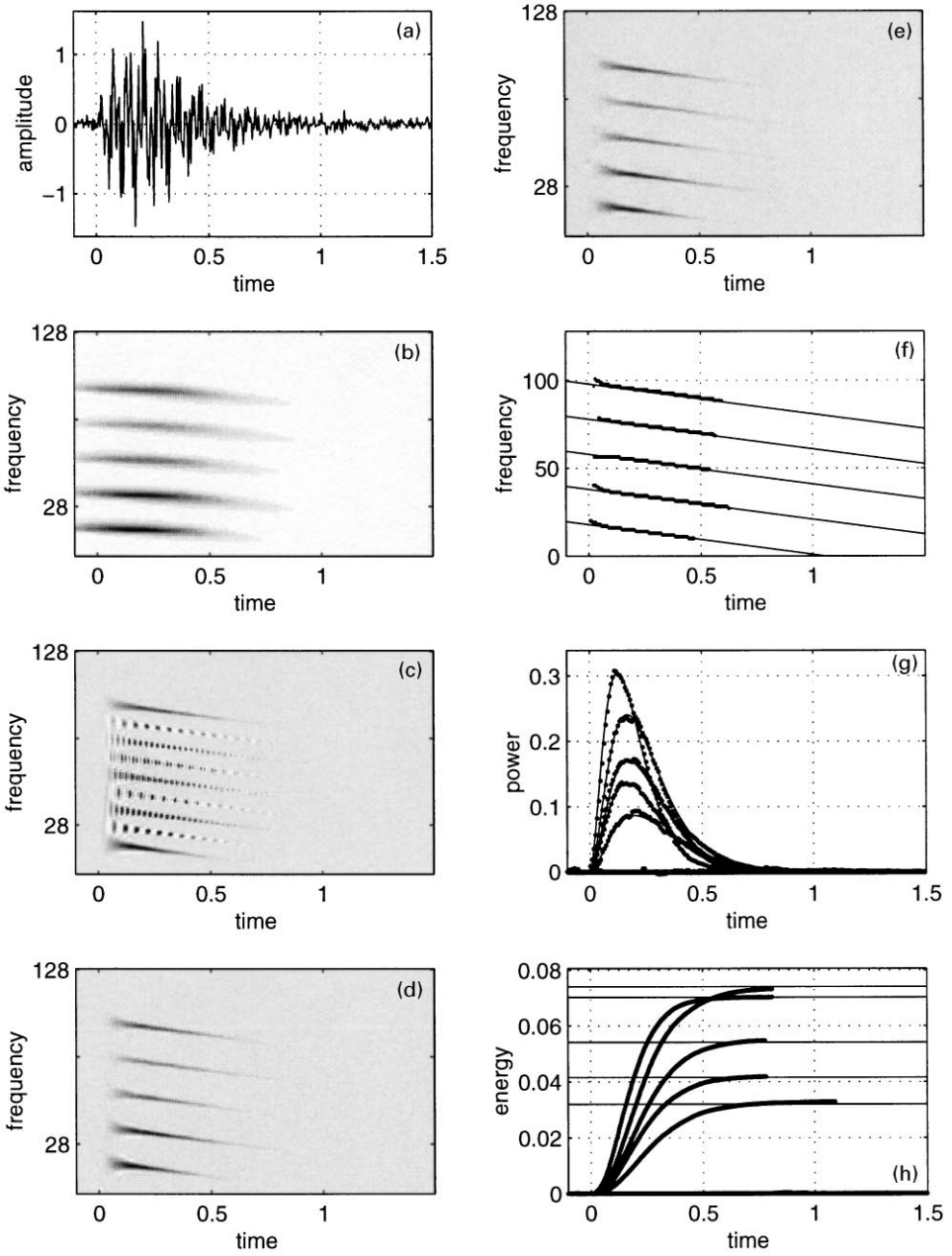

Fig. 1. Time–frequency analysis of the simulated pressure or sound signal: (a) signal in the time domain; (b) spectrogram; (c) Wigner distribution; (d) sum of the Wigner distributions calculated for each signal component separately, in (c) the same gray scale is used as in (d); (e) time–frequency representation using the S-method with $L_P = 4$; (f) instantaneous frequencies: exact (line), calculated using the time–frequency representation (e) (thick line); (g) components power: exact (line), calculated using the time–frequency representation (dotted); (h) components energy (line), cumulative component powers calculated using the time–frequency representation (thick line). Reference level is determined by $Q^2 = 200$. The lag window $w(\tau)$ is the same for all distributions.

4.2. Experimental data

The procedure which has been presented in the paper and tested on a synthetic signal is applied to sound and pressure signals of a 6-cylinder BMW test bed engine measured in parallel at different speeds: 1000 rpm, 2000 rpm and 5000 rpm.[2]

As in the cases of the synthetic signals, the signals themselves, their time–frequency representations using the S-method, instantaneous frequencies, powers, and cumulative powers corresponding to the selected pressure and sound at speed 1000 rpm are shown in Fig. 2. Both pressure and sound signals are highly nonstationary signals with the significant oscillations starting just after 10° crank angle. Crank angle is measured in degrees from top dead center (TDC). In the sound signal, Fig. 2(d-right), the algorithm recognized four separate components also just after 10° crank angle. The power calculated prior that angle is assigned to one component only and is located between two components with higher instantaneous frequencies (Figs. 2(c,d-right)). The energies of oscillations in both, pressure signal and sound signal are mainly located along three resonance time-varying frequencies. While in the pressure signal the energy is mostly concentrated in the middle component, in the sound signal the energy is mainly concentrated in the two other dominant components. In the pressure signal the dominant part of energy is located up to the crank angle just higher than 20°, while the oscillations in the sound signal last longer, up to a crank angle of about 35°. The linear frequency modulation corresponding to temperature variations is especially notable on the longer lasting sound signal (Fig. 2(c-right)). It is easy to estimate that the instantaneous frequency law, e.g., for the middle frequency component is

$$\varphi'(t) = -0.09\theta + 13.125 \text{ kHz},$$

where θ denotes the crank angle in degrees from TDC that is a time integral over speed. We can also observe that the middle resonance frequency in the sound signal, corresponding to the strongest oscillation in the pressure signal, has significant power variations. A small resonance between two higher strong resonance components appeared in the sound signal as well. Most of these effects can be considered as a consequence of the existing evidences that the sound signal $y(t)$ can be seen as a time-variant filtered noisy version of the pressure signal $x(t)$,

$$y(t) = \int_{-\infty}^{t} h(t, t-\tau)x(\tau)\,\mathrm{d}\tau + n(t),$$

and the time variance of h depends on t over crank angle θ only.

In the case of experimental data we are not able to check directly the proposed algorithm and the calculation procedure, as in the case of simulated signals. But few rough check points can be indicated in the real data cases as well. If we have obtained correct results, we can expect for example that the following relation for the signal and calculated powers $|A_p(t)|^2$ holds:

$$|y(t)| \leqslant 2\sum_{p=1}^{P} |A_p(t)|,$$

with equality for the points where all components in Eq. (21) are in phase $\varphi_p(t) = k\pi$. Considering, for example, the sound signal in Fig. 2(a-right) we can see a strong negative peak at 15^0 crank angle. A high possibility is that the existing four components summed at this point in phase producing a sum of amplitudes. Calculating the amplitudes as square roots of the powers from Fig. 2(d-right) at $\theta = 15^\circ$ we roughly get $2\sum_{i=1}^{P} A_p(t) = 2(\sqrt{400} + \sqrt{320} + \sqrt{250} + \sqrt{90}) = 1060$, what is in good agreement with the amplitude in Fig. 2(a-right). Once more we want to emphasize that this is a quite rough check. It can be influenced by the existing noise as well as by the fact that the components of a multicomponent signal very rarely take the same multiple of π phase. The procedure for the energy calculation can be easily checked by comparing the area under a power curve and the corresponding energy. For example, the highest power component in Fig. 2(d-right) has the area of about $1\frac{1}{3} \times [10^\circ \times 2 \cdot 10^4]$, where 10° means 10 degree crank angle. One crank angle degree corresponds to $1.666 \cdot 10^{-4}$ sec for a speed of 1000 rpm. Therefore the energy should be about 45 units that corresponds

[2] Support of the ARAL Research, Bochum is acknowledged.

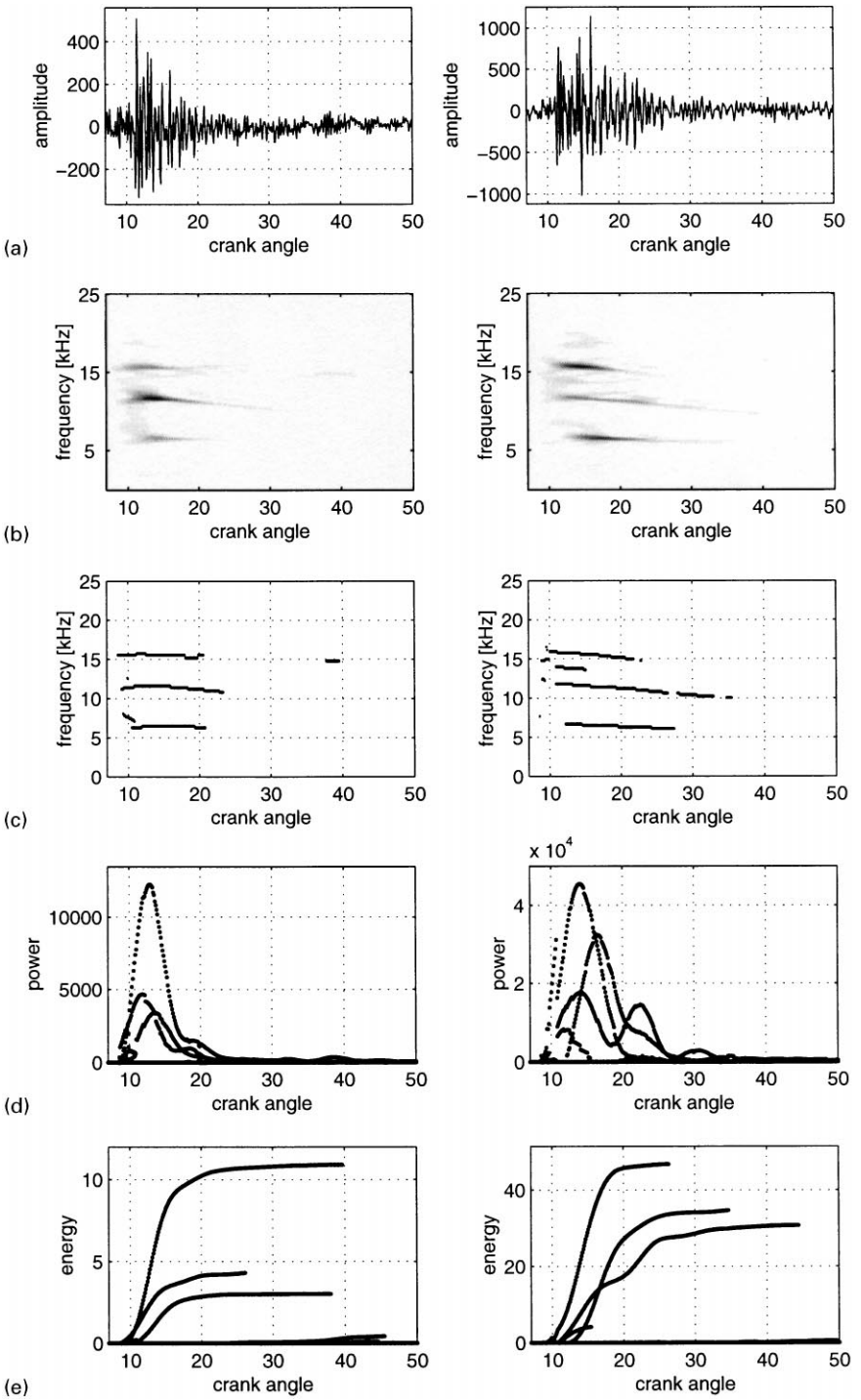

Fig. 2. Time–frequency analysis of the pressure signal (left) and sound signal (right) with speed 1000 rev/min: (a) signal in the time domain, (b) time–frequency representation using the S-method with $L_P = 2$, (c) instantaneous frequencies, (d) components' power, (e) components' cumulative power. Reference level is determined by $Q^2 = 100$. Time is measured in crank angle degrees from the TDC.

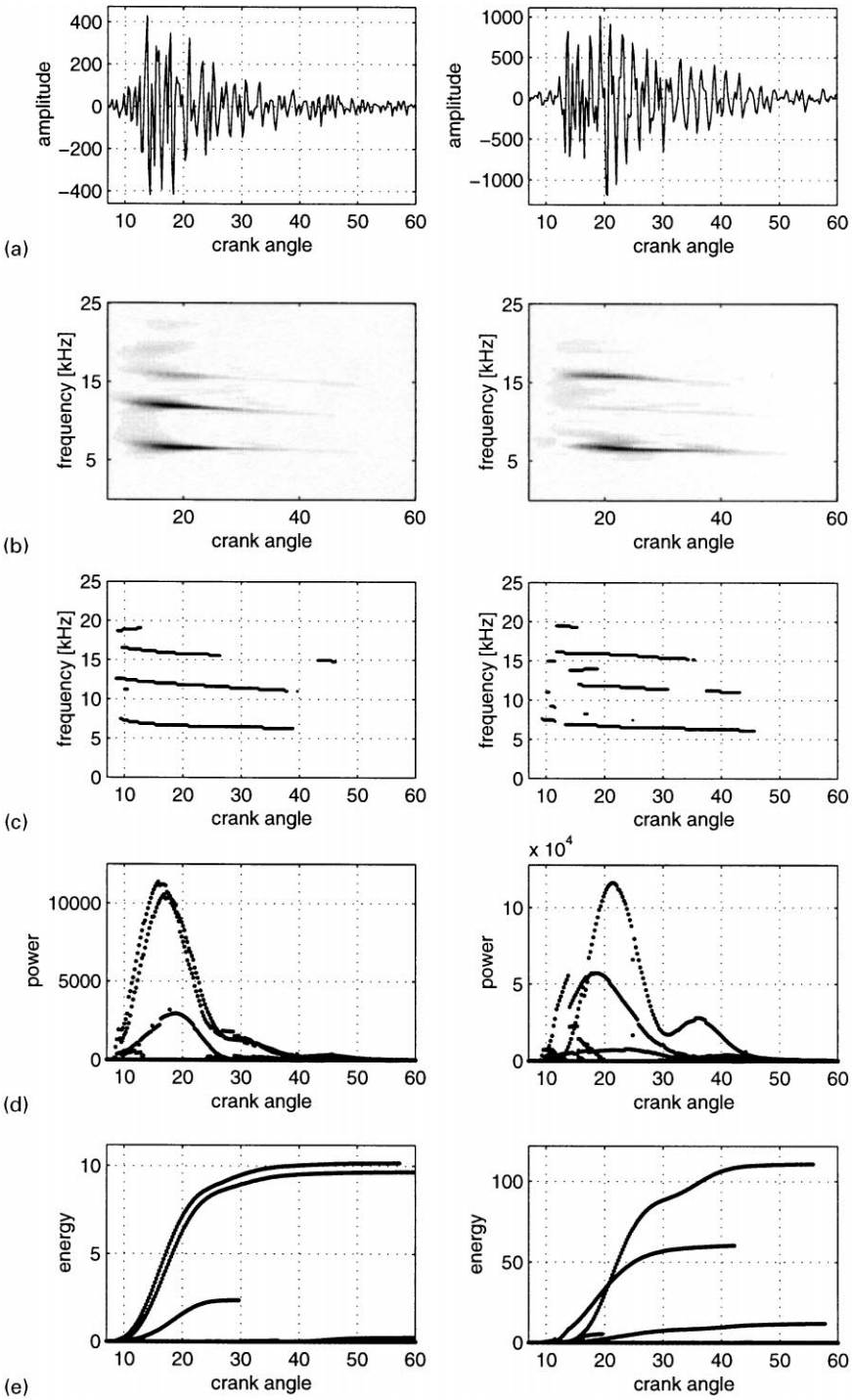

Fig. 3. Time–frequency analysis of the pressure signal (left) and sound signal (right) with speed 2000 rev/min: (a) signal in the time domain, (b) time–frequency representation using the S-method with $L_P = 2$, (c) instantaneous frequencies, (d) components' power, (e) components' cumulative power. Reference level is determined by $Q^2 = 100$. Time is measured in crank angle degrees from the TDC.

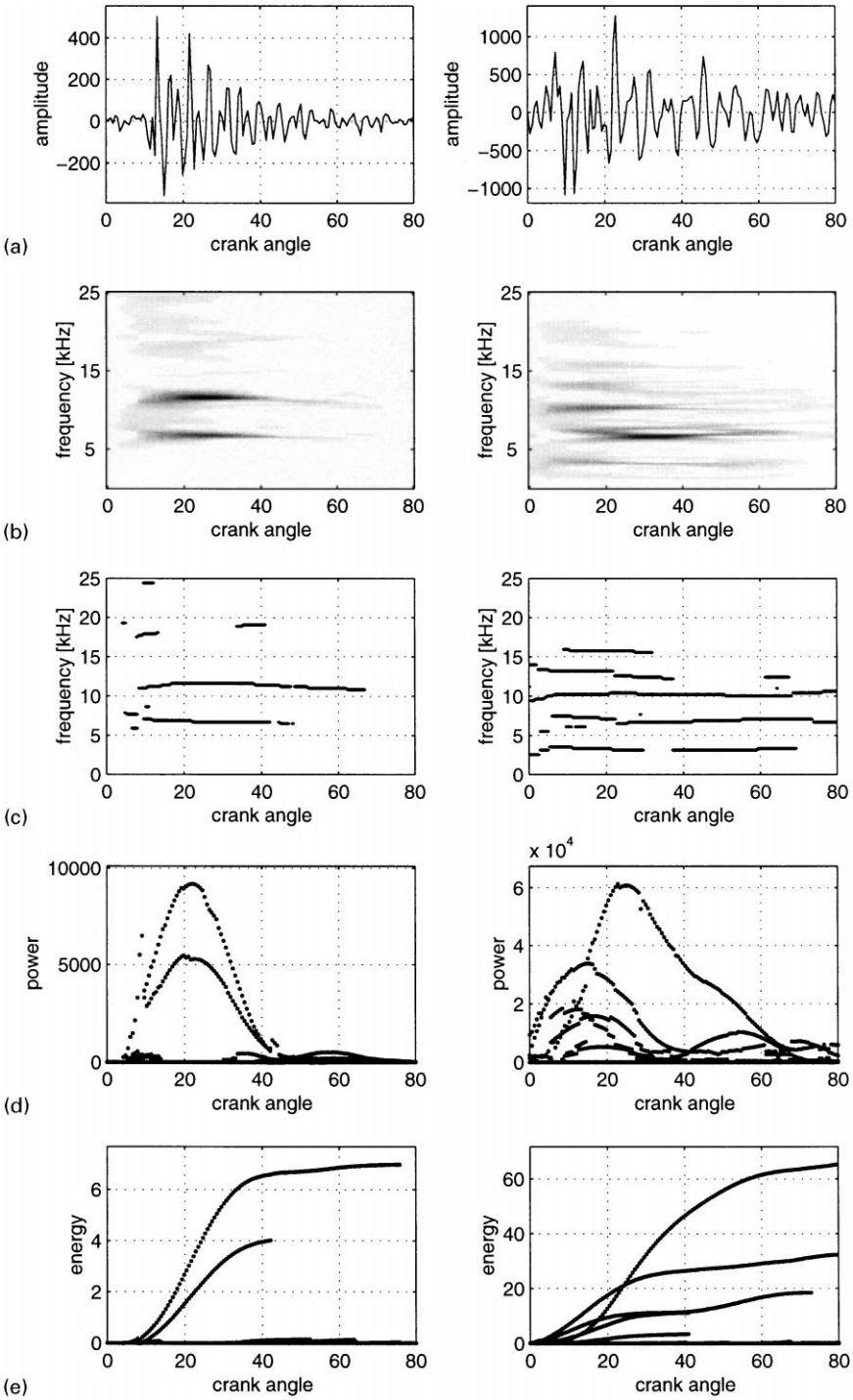

Fig. 4. Time–frequency analysis of the pressure signal (left) and sound signal (right) with speed 5000 rev/min: (a) signal in the time domain, (b) time–frequency representation using the S-method with $L_P = 2$, (c) instantaneous frequencies, (d) components' power, (e) components' cumulative power. Reference level is determined by $Q^2 = 100$. Time is measured in crank angle degrees from the TDC.

to the value in Fig. 2(e-right). The power calculation along with its cumulative form producing resonance energies is a good indicator for the knock detection.

Results of the time–frequency analysis of pressure and sound signals measured at the speed of 2000 rpm are shown in Fig. 3. The energy of the pressure signal is located in two lower frequency components, while that of the sound signals is mainly located in the lowest and highest component. The middle component in the pressure signal almost disappeared in the sound signal. Changes of the power of the lowest frequency component in the sound signal, having almost constant frequency, shows that the transfer function from pressure signal to the sound signal is highly time-variant. Similar amplitude and energy check as in the previous case can be made. An interesting point for the amplitude check is in the sound signal at the crank angle of 20°.

Sound and pressure signals measured at a high speed of 5000 rpm are analyzed in Fig. 4. For this case we can first note that the sound signal is strongly corrupted by the noise. The oscillations starting point can hardly be observed in the sound signal due to noise. But if we concentrate only on the energy of the strongest component, then we can conclude that it starts just about crank angle of 10°, the same as the oscillations in the pressure signal. Also we can conclude that there are two dominant components in the sound signal at almost the same frequency positions as in the pressure signal, while the third strongest component appeared at a very low frequency where there was not any significant component in the pressure signal.

5. Conclusion

An analysis of multiple resonances in combustion engine signals is done. It is based on the S-method that can produce a time–frequency representation equal to the sum of the pseudo-Wigner distributions of each signal component separately. Some new theoretical aspects of this method are presented. In the analysis only one signal realization is used. Basic step for the realization of the S-method is the short-time Fourier transform calculation. It can be done using efficient FFT algorithms or recursive approaches that require few additions and multiplications for each time instant and frequency and can be performed in parallel. The S-method realization only requires some additional multiplications and additions that can also be performed for each time–frequency point in parallel. Therefore, numerically efficient realizations of the method are possible, including hardware online realization. Time–frequency representations produced by the S-method are used to calculate instantaneous frequencies and energies of each pressure and sound signal component. These two parameters are important for the knock detection. The accuracy of the obtained results is checked on synthetic signals. The method is then applied to several real data examples. Some rough checks for the real data analysis are proposed and performed.

The presented pressure signal and corresponding sound signal analysis can be used in several research and application directions. There exist strong evidences that the sound signals are obtained as noisy time-varying filtered versions of the pressure signals. The results presented in this paper can be used to test the mathematical models of the system transfer functions from the pressure to the sound signals. After a reliable relation between these signals has been established, then only sound signals, i.e. their parameters as studied in the paper, can be used in combustion observation. The powers of the sound signal resonances calculated according to the procedure presented in the paper and related to the energies of the pressure signal resonances, can be used for knock detection. Instantaneous frequencies that follow from the described procedure are important parameters as they indicate the temperature changes in the combustion chamber.

References

[1] J.B. Allen, L.R. Rabiner, A unified approach to short-time Fourier analysis and synthesis, Proc. IEEE 65 (November 1977) 1558–1564.

[2] M.G. Amin, A new approach to recursive Fourier transform, Proc. IEEE 75 (1987) 1357–1358.

[3] J.F. Böhme, D. König, Statistical processing of car engine signals for combustion diagnosis, in: Proc. IEEE 7th

Workshop on Statistical Signal and Array Processing, Quebec, 1994, pp. 369–374.
[4] T.M. Bossmeyer, D.J. Hansknecht, D. König, Time–frequency analysis of knock in spark ignition engines, in: Proc. EUSIPCO, Brussels, 1992, pp. 1765–1768.
[5] O.Boubal, J. Oksman, Application de la distribution de pseudo Wigner–Ville lissée réallouée à la détection de cliquetis, Traitement du Signal, submitted.
[6] L. Cohen, Time–Frequency Signal Analysis, McGraw Hill, 1995.
[7] L. Cohen, Distributions concentrated along the instantaneous frequency, SPIE 1348 (1992) 149–157.
[8] N. Härle, J.F. Böhme, Detection of knocking for spark ignition engines based on structural sounds, in: Proc. IEEE-ASSP, Dallas, 1987, pp. 1744–1747.
[9] R. Hickling, D.A. Feldmair, F.H.K. Chen, J.S. Morel, Cavity resonances in engine combustion chambers and some applications, J. Acoust. Soc. Amer. 73 (1983) 1170–1178.
[10] F. Hlawatsch, G.F. Boudreaux-Bartels, Linear and quadratic time-frequency signal representations, IEEE Signal Processing Mag. (April 1992) 21–67.
[11] I. Djurović, LJ. Stanković, A virtual instrument for time-frequency signal analysis, IEEE Instrumentation and Measurements, December 1999, to appear.
[12] V. Katkovnik, LJ. Stanković, Instantaneous frequency estimation using the Wigner distribution with time-varying and data-driven window length, IEEE Trans. Signal Process. 46 (9) (September 1998) 2315–2325.
[13] D. König, J.F. Böhme, Application of cyclostationary and time-frequency signal analysis to car engine diagnosis, in: Proc. IEEE-ICASSP, Adelaide, 1994, pp. 149–152.
[14] D. König, J.F. Böhme, Wigner–Ville spectral analysis of automotive signals captured at knock, Applied Signal Processing 3 (1996) 54–64.
[15] D. König, Analyse nichstationärer Triebwerkssignale insbesondere solcher klopfender Betriebszustände, Dr.-Ing. dissertation, Ruhr Universität Bochum, VDI Verlag, 1995.
[16] K.J.R. Liu, Novel parallel architecture for short time Fourier transform, IEEE Trans. CAS-II 40 (December 1993) 786–789.
[17] G. Matz, F. Hlawatsch, W. Kozek, Generalized evolutionary spectral analysis and the Wey Spectrum of nonstationary random processes, IEEE Trans. Signal Process. 45 (June 1997) 1520–1534.
[18] F. Molinaro, F. Castanie, A comparison of time-frequency models, in: Proc. EUSIPCO, Barcelona, 1990, pp. 145–148.
[19] LJ. Stanković, A method for time-frequency analysis, IEEE Trans. Signal Process. 42 (January 1994) 225–229.
[20] LJ. Stanković, A multitime definition of the Wigner higher order distribution: L-Wigner distribution, IEEE Signal Process. Lett. 1 (July 1994) 106–109.
[21] LJ. Stanković, Auto-term representation by the reduced interference distributions: The procedure for a kernel design, IEEE Trans. Signal Process. 44 (June 1996) 1557–1564.
[22] LJ. Stanković, Highly concentrated time-frequency distribution: Pseudo quantum signal representation, IEEE Trans. Signal Process. 45 (March 1997) 543–551.
[23] S. Stanković, LJ. Stanković, An architecture for the realization of a system for time-frequency analysis, IEEE Trans. Circuits and Systems-II 44 (July 1997) 600–604.
[24] LJ. Stanković, S. Stanković, On the Wigner distribution of the discrete-time noisy signals with application to the study of quantization effects, IEEE Trans. Signal Process. 42 (7) (July 1994) 1863–1867.
[25] M. Wagner, Karlsson, D. König, C. Törk, Time variant system identification for car engine signals, in: Proc. EUSIPCO, Edinbourgh, 1994, pp. 1409–1412.